TOPOGRAPHIC CONTROLS ON STOMATAL AND MESOPHYLL LIMITATIONS TO PHOTOSYNTHESIS IN TWO SUBALPINE CONIFERS

Jiemin Guo,[1,*] Daniel P. Beverly,* Jason J. Mercer,* Craig S. Cook,† Brent E. Ewers,* and David G. Williams*,‡

*Department of Botany, University of Wyoming, Laramie, Wyoming 82071, USA; †Stable Isotope Facility, University of Wyoming, Laramie, Wyoming 82071, USA; and ‡Department of Ecosystem Science and Management, University of Wyoming, Laramie, Wyoming 82071, USA

Editor: Barry A. Logan

Premise of research. Leaf stomatal and mesophyll conductances limit photosynthesis and influence water use efficiency. Few studies have quantified the relative limitations imposed by these CO_2 diffusion pathways on photosynthesis in mature conifer trees under natural conditions. Here, we report observations of stomatal and mesophyll conductance changes during seasonal drying across contrasting topographic positions in two Rocky Mountain conifers. We predicted that topographic controls on soil water availability and energy balance would determine limitations to photosynthesis by mesophyll conductance across conifer species with contrasting patterns of stomatal and hydraulic traits.

Methodology. Concurrent measurements of leaf gas exchange and carbon isotope discrimination were used to estimate stomatal (g_s) and mesophyll (g_m) conductance in branches of an isohydric species, lodgepole pine (*Pinus contorta*), and an anisohydric species, Engelmann spruce (*Picea engelmannii*), in the central Rocky Mountains. Quantitative limitation analysis of photosynthesis (A) was then performed using data from CO_2 response curves.

Pivotal results. Stomatal conductance imposed greater limitations on photosynthesis (42%–67%) than mesophyll conductance (5%–17%), but no significant differences in g_m were observed between the two conifer species. At the mesic lower hillslope position, A, g_s, and g_m increased during the growing season despite declines in soil moisture. In contrast, at the drier upper hillslope position, declines in soil moisture and increases in air temperature during the growing season are correlated with reductions in g_s but not with A or g_m.

Conclusions. Adjustments in g_m played a potentially important role in sustaining photosynthesis and improving plant water use efficiency when stomatal conductance decreased with water limitation during the growing season at the research site. Sustained g_m with seasonal drought may be an important mechanism allowing conifers to survive and maintain competitive dominance in low-resource habitats.

Keywords: mesophyll conductance, *Pinus contorta*, *Picea engelmannii*, soil moisture, ^{13}C discrimination, water use efficiency.

Online enhancements: supplemental information, tables, and figures.

Introduction

Plants avoid desiccation and excessive xylem tensions by reducing stomatal conductance (g_s) and transpiration during periods of high evaporative demand and limited water supply from roots (Sperry 2000; Brodribb and Holbrook 2003; Sevanto et al. 2018). Reductions in g_s limit CO_2 diffusion into intercellular air spaces, potentially lowering the photosynthetic rate (A) when CO_2 is not saturating (Buckley 2005). Conductance of CO_2 along the diffusion pathway inside leaves (mesophyll conductance [g_m]) colimits the supply of CO_2 for photosynthesis but does not directly affect the transpiration rate at the leaf surface (Evans and von Caemmerer 1996; Flexas et al. 2012, 2013*a*, 2013*b*; Gago et al. 2019). Therefore, sustained or increased A and intrinsic water use efficiency (iWUE; A/g_s) could be achieved by reducing diffusion limitations imposed by mesophyll conductance (Grassi and Magnani 2005; Flexas et al. 2008, 2016; Tholen and Zhu 2011).

Covariation between g_s and g_m and their limitations on photosynthesis and influence on water use efficiency are poorly

[1] Author for correspondence; email: jiemin2014@gmail.com.

Manuscript received January 2021; revised manuscript received October 2021; electronically published January 27, 2022.

International Journal of Plant Sciences, volume 183, number 3, March/April 2022. Published by The University of Chicago Press. https://doi.org/10.1086/718050

documented under natural conditions (Flexas et al. 2016; Sevanto et al. 2018). Stomatal and mesophyll conductances are often similar in magnitude (Warren 2008*b*), and both have been observed to limit photosynthetic rate and influence leaf-level water use efficiency (Duan et al. 2011; Cano et al. 2013; Flexas et al. 2013*a*). However, the proportionality of these limitations likely varies across species (Peguero-Pina et al. 2012), and each conductance may have separate sensitivities to changes in the environment (Flexas et al. 2012).

Stomatal responses to leaf water supply and transpiration demand may have varying impacts on photosynthesis and water-use efficiency depending on correlated responses of mesophyll conductance (Dewar et al. 2018). Isohydric species maintain relatively constant midday minimum water potentials to avoid drought-induced hydraulic damage by reducing stomatal conductance and transpiration as soil water availability declines. In these species where water limitations arise, strong coordinated changes in mesophyll conductance might offset stomatal limitations to CO_2 uptake. In contrast, anisohydric species sustain relatively high stomatal conductance as midday leaf water potential drops, allowing CO_2 fixation to continue to a certain degree but with greater risk of xylem cavitation (McDowell et al. 2008). In species that display a more anisohydric behavior, the overriding adjustments of mesophyll conductance might be important only for sustaining adequate supply of CO_2 to chloroplasts during drought since stomata remain relatively open. The conifer species chosen for the present study express isohydric (*Pinus contorta*) and anisohydric (*Picea engelmannii*) stomatal regulation.

Conifers, which display a wide range of hydraulic traits and stomatal behaviors, dominate forests at high northern latitudes and in cool and dry montane environments (Woodward 1995). In the Rocky Mountains of North America, conifers exist across contrasting topographic positions and over broad elevational ranges spanning habitats with highly variable and seasonally contrasting soil water availability. The magnitude of g_m relative to g_s in conifers and the proportional responses of g_m and g_s to these contrasting patterns of water availability could have important implications for modeling photosynthesis at the global scale (Bonan 2019). Conifers are reported to have low g_m caused by thick cell walls and the chloroplasts' alignment against intercellular air space (Veromann-Jürgenson et al. 2017, 2020; Kooijmans et al. 2019), but only a few studies have quantified mesophyll conductance in mature conifer trees under natural conditions (Warren et al. 2003; Wingate et al. 2007; Bickford et al. 2010; Ubierna and Marshall 2011; Stangl et al. 2019), particularly over contrasting topographic positions where steep gradients of soil moisture availability, temperature, and vapor pressure deficit (VPD) develop. Most studies on g_m responses to water limitation in conifers have been carried out on potted seedlings in controlled environments, which may not accurately represent responses of g_m to water limitations in mature trees in the field. The relationship between temperature, VPD, and g_m under natural conditions has yet to be investigated. In the current study we measured photosynthetic rate and stomatal and mesophyll conductances in branches of adult conifer trees of two species with contrasting patterns of stomatal regulation (lodgepole pine, *P. contorta*, and Engelmann spruce, *P. engelmannii*) in the Medicine Bow Range west of Laramie, Wyoming. We measured these traits in branches from trees at upper and lower positions on a south-facing hillslope where differences in soil depth, site energy balance, and drainage source area create potentially large contrasts in available soil moisture, especially late in the growing season.

We addressed the following questions. First, what is the magnitude of mesophyll conductance in *P. contorta* and *P. engelmannii*, and how does this trait respond to decreasing soil moisture under natural conditions? To what degree does the mesophyll conductance response differ between the more isohydric and more anisohydric conifer species studied? Second, what is the relative limitation to photosynthesis by g_m compared with g_s under different moisture conditions? And third, how do variations in stomatal and mesophyll conductances influence iWUE?

Material and Methods

Field Site Description

Twig samples were collected from mature Engelmann spruce (*Picea engelmannii*) and lodgepole pine (*Pinus contorta*) trees in the Medicine Bow Mountains of southeastern Wyoming. These two conifers, together with subalpine fir (*Abies lasiocarpa*), represent the dominant tree cover in subalpine forests over much of the central Rocky Mountains. We sampled at two field sites over the growing season (June–September) of 2015 in the No-Name Watershed (120-ha catchment, 3000 m asl, lat. 41°20′N, long. 106°20′W) along a south-facing hillslope gradient. The climate at our field sites is defined by long, cold winters and short, dry summers, with substantial winter snowfall (mid-October through May) followed by an extended dry growing season. Average annual precipitation at these field sites is about 1000 mm, with three-fourths of the precipitation occurring as snow, and mean annual air temperature is 1.5°C. The "upper hillslope" site is on the upper portion of a south-facing slope where the drainage source area is small and soils are shallow and rocky. The "lower hillslope" site is at the base of the south-facing slope fed by a larger drainage area, and the soils are generally deeper and store more water compared with the upper hillslope areas (Thayer et al. 2018). The upper and lower hillslope sites are approximately 300 m apart with 50 m of elevation difference.

Soil Moisture, Temperature, VPD, and Leaf Water Potential Measurements

Volumetric soil water content (θ) was continuously recorded in 2015 using CS625 soil moisture probes (Campbell Scientific) installed vertically at depths of 10 and 50 cm at each sample site. Soil water content data were recorded every 30 min using a CR1000 data logger (Campbell Scientific). Predawn and midday leaf water potentials (Ψ_{pd}, Ψ_{md}) were determined using a Scholander pressure chamber (PMS Instrument) on twigs from the same trees and canopy positions used for the gas exchange and on-line ^{13}C discrimination measurements described below. Meteorological data were obtained from a weather station at the field site. The mean temperature and VPD during the growing season were calculated and are shown in figure 1. Mean daily temperatures and daily maximum VPD over 7 d prior to each measurement were used as indexes of growth conditions to test their relationship with g_m.

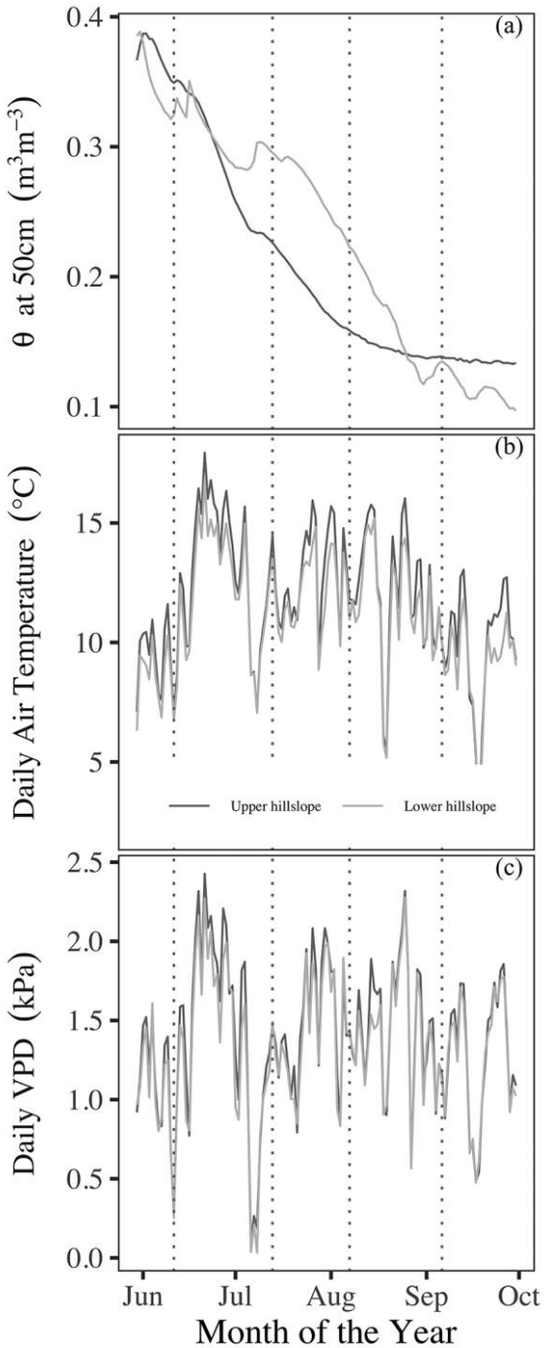

Fig. 1 Daily soil moisture reported as water volume relative to soil volume (θ; $m^3\ m^{-3}$) at 50-cm soil depths, temperature, and maximum vapor pressure deficit (VPD) at upper and lower hillslope sites.

Gas Exchange and On-Line ^{13}C Discrimination Measurements

Concurrent measurements of leaf gas exchange and photosynthetic carbon isotope discrimination provide one means to estimate g_m under a range of conditions (Evans et al. 1986; Barbour et al. 2010, 2016; Ogée et al. 2018; Stangl et al. 2019). We sampled branches from the upper sunlit portion of the canopy for measurements each month from June to September in 2015. Branches from four *P. contorta* and four *P. engelmannii* trees were collected at each of the two sites from the same trees over every sampling campaign. We followed the sampling and handling procedures for branches reported in Monson et al. (2005). Branches were harvested before dawn and then transported (transit time of about 1 h) to the lab in an insulated cooler with wet paper towels in sealed plastic bags for measurement on the same day. Branch stems were recut underwater, and the freshly cut end was kept submerged during gas exchange measurements. The terminal section of a single twig on each branch was placed into a gas exchange chamber fitted to a photosynthesis analyzer (LI 6400XT IRGA and conifer chamber, LI-COR, Lincoln, NE). Needle leaf area was estimated with projected leaf area with a flatbed scanner and ImageJ software (http://rsb.info.nih.gov/ij/, US National Institutes of Health). Gas exchange measurements were made under saturating light with a red-green-blue LED light source, with equal intensities of each color light (PPFD = 1500 μmol m^{-2} s^{-1}; LI 6400-18 RGB Light Source). Sample CO_2 concentration was set at 400 ppm. Flow rate was controlled between 200 and 400 μmol s^{-1} to maintain a sufficient CO_2 drawdown between the reference and sample gas streams. We assumed that the air surrounding the leaf was well mixed inside the chamber and that the boundary layer resistance was negligible, and therefore the default value was used for this study. For all the measurements, the CO_2 drawdown was greater than 65 μmol mol^{-1}. Relative humidity was maintained between 50% and 75%, and chamber temperature was set at 25°C. We calibrated the IRGA in the morning of each measurement day and matched the reference and sample gas analyzers of the IRGA prior to each measurement cycle. After we placed twigs inside the chamber, we gave the needles 15 min to adjust to the chamber conditions before measurements. Measurements were recorded every 10 s for ~8 min.

The gas exchange system was coupled to an isotope ratio midinfrared spectrometer (Delta Ray, Thermo Fisher Scientific) to measure photosynthetic carbon isotope discrimination (Δ_{obs}) under the conditions described above. Pure CO_2 with a known isotopic composition was supplied to the LI 6400 IRGA as source CO_2; the $\delta^{13}C$ value of this gas was -16.2 ± 0.006‰ (Vienna Pee Dee Belemnite [VPDB]) for measurements made in June and -12.3 ± 0.005‰ for all other measurements, which were calibrated against a CO_2 standard gas (Oztech) on a dual inlet MAT 253 IRMS (Thermo Fisher Scientific) at the University of Utah's Stable Isotope Ratio Facility for Environmental Research. The gas streams of the reference gas entering the leaf chamber and the sample gas leaving the chamber after exchange with leaves inside the chamber were routed into the Delta Ray using Teflon tubing with two Swagelok T fittings. After connecting the Delta Ray inlet tubes with the IRGA, we leak tested during the later period of the 15-min adjusting period by blowing high-CO_2 air (from human breath) gently around the chamber and switching connections along the flow paths. With no observable disruptions in CO_2 concentration and $\delta^{13}C$ values recorded on the Delta Ray, we assumed that there was no leaking in the system (Bickford et al. 2009). The gas samples were dried with the instrument's internal Nafion drier before they entered the laser measurement cell. The Delta Ray measured

concentrations of the CO_2 isotopologues $^{13}CO_2$ and $^{12}CO_2$ in the reference and sample gases. Each measurement cycle lasted for ~8 min after a 45-s flushing with the incoming measurement gas stream. The 8-min measurement cycle consisted of alternating 1-min cycles recording the isotopic composition of calibration, reference, and sample gases from the LI 6400 portable photosynthesis system.

The laser of the Delta Ray scanned over absorption lines at 500 Hz, and then the signal was averaged for 1 s before the spectrum was fitted and isotope ratios were calculated from the spectrum fit from the Delta Ray software. Measured isotope ratios were referenced to the VPDB scale using a two-point calibration derived from calibrated CO_2 reference gases with high and low isotope ratio values. The two working standard gases used in our measurements were made by mixing the pure CO_2 with synthetic air in 116-L aluminum gas cylinders in the University of Wyoming Stable Isotope Facility. These gases were calibrated against a CO_2 standard gas (Oztech) on a dual inlet MAT 253 IRMS (Thermo Fisher Scientific) at the University of Utah's Stable Isotope Ratio Facility for Environmental Research. The CO_2 concentrations for the two working standard gases were 414.05 ± 1.30 μmol mol^{-1} and 418.52 μmol mol^{-1}, respectively ($n = 4$). The $\delta^{13}C$ values were −10.74 ± 0.02‰ and −26.88 ± 0.20‰ ($n = 4$). The standard deviation of the $\delta^{13}C$ values measured on "working standard gas1" using the Delta Ray ranged from 0.07‰ to 0.10‰ over each measurement day. We evaluated the degree that the gas exchange instrument would cause isotope fractionations by measuring the reference and sample gas streams passing through an empty leaf chamber; the differences between reference and sample gases during these tests were <0.2‰. These small differences near the confidence limits for estimates of international reference materials for $\delta^{13}C$ calibration were ignored in further calculations and corrections of our data.

Calculations of ^{13}C Discrimination and Mesophyll Conductance

The instantaneous ^{13}C discrimination occurring during gas exchange was calculated as (Evans et al. 1986)

$$\Delta_{obs} = \frac{\xi(\delta_o - \delta_e)}{1 + \delta_o - \xi(\delta_o - \xi_e)} \tag{1}$$

and

$$\xi = \frac{c_e}{c_e - c_o}, \tag{2}$$

where c_e and δ_e are concentrations and $\delta^{13}C$ values of CO_2 entering the leaf chamber and c_o and δ_o are those for CO_2 leaving the leaf chamber after exchange with leaves inside (for a definition of terms, see the supplemental information, available online). We maximized the amount of leaf area inside the leaf gas exchange chamber and adjusted flow rates to maximize ^{13}C discrimination and CO_2 drawdown to reduce uncertainty in our estimates of g_m. We excluded measurements from the data set for further analysis and calculations if the difference between δ_o and δ_e was less than 1‰, $c_e - c_o$ was less than 30 μmol mol^{-1}, or ξ was greater than 10 (table 1; Bickford et al. 2010).

We estimated g_m from the difference between calculated carbon isotope discrimination, assuming infinite g_m (Δ_i, eq. [3]), and that measured (Δ_{obs}, eq. [1]; Barbour et al. 2010; Farquhar and Cernusak 2012)

Table 1

Range and Mean (SD) of Measured Values Used for the Determination of Mesophyll Conductance Using the Instantaneous ^{13}C Discrimination Technique after Filtering Data Not Meeting Quality Control Thresholds as Described by Bickford et al. (2010)

	Min	Max	Mean (SD)
$c_e - c_o$ (μmol mol^{-1})	53.5	212	113 (32)
$\delta_o - \delta_e$ (‰)	1.20	3.5	2.44 (.56)
ξ	2.88	8.50	4.80 (1.1)

Note. Values are the difference in CO_2 concentration ($c_e - c_o$) and $\delta^{13}C$ ($\delta_o - \delta_e$) between gas entering (c_e, δ_e) and leaving (c_o, δ_o) the leaf chamber, and ξ is calculated from equation (2).

$$\Delta_i = \frac{1}{1-t}\left[a_b\frac{C_a - C_s}{C_a} + a_s\frac{C_s - C_i}{C_a}\right] + \frac{1+t}{1-t}\left[b\frac{C_i}{C_a} - \frac{\alpha_b}{\alpha_{e'}}e'\frac{R_d}{A+R_d}\frac{C_i - \Gamma^*}{C_a} - \frac{\alpha_b}{\alpha_f}f\frac{\Gamma^*}{C_a}\right], \tag{3}$$

where C_a, C_s, and C_i are the ambient, leaf surface, and intercellular CO_2 concentrations (μmol mol^{-1}); a_b and a_s are the fractionations occurring during diffusion through the leaf boundary layer (2.9‰; Evans et al. 1986) and the stomata (4.4‰; Farquhar and Richards 1984); b is the fractionation associated with Rubisco carboxylation (29‰; Roeske and O'Leary 1984); f is the fractionation associated with photorespiration (16.2‰ was used for this study; Wingate et al. 2007; Evans and von Caemmerer 2013); and e' is the fractionation associated with day respiration, taking into account the ^{13}C disequilibrium between atmospheric and tank CO_2 (Tazoe et al. 2011). We assumed no fractionation by day respiration, and e' was calculated as $\delta^{13}C_{tank} - \delta^{13}C_{atm}$; $\delta^{13}C_{tank}$ for this study was −16.2‰ (June) and −12.3‰ (other 3 mo). It was assumed that $\delta^{13}C_{atm}$ was −8‰, α_b is the fractionation factor for carboxylation ($1 + b$), $\alpha_{e'}$ is the fractionation factor for day respiration ($1 + e'$), α_f is the fractionation factor for photorespiration ($1 + f$), and R_d is the rate of day respiration and was assumed to be 0.9 (μmol m^{-2} s^{-1}). The photosynthetic rate is A; Γ^* is the compensation point in the absence of day respiration and was assumed to be 45 μmol mol^{-1} (Bernacchi et al. 2002).

The ternary correction accounts for effects of transpiration on the rate of CO_2 fixation through stomata and is defined as (von Caemmerer and Farquhar 1981; Farquhar and Cernusak 2012)

$$t = \frac{\alpha_{ac}E}{2g_{ac}}, \tag{4}$$

where E is the transpiration rate (mmol H_2O m^{-2} s^{-1}), g_{ac} is the total conductance of CO_2 diffusion through the stomata and the boundary layer (μmol m^{-2} s^{-1}), and α_{ac} is the fractionation factor of CO_2 diffusion ($1 + \bar{a}$), where $\bar{a}$ is the weighted fractionation attributable to diffusion through the leaf boundary layer and the stomata in series (Evans et al. 1986; Cernusak et al. 2013):

$$\frac{a_b(C_a - C_s) + a_s(C_s - C_i)}{(C_a - C_i)}. \quad (5)$$

We then estimate g_m by the difference between predicted Δ_i (where CO_2 concentration in the chloroplast $[C_c] = C_i$) and Δ_{obs}, as given by Farquhar and Cernusak (2012):

$$\frac{1+t}{1-t}\frac{\left(b - a_m - \frac{\alpha_b}{\alpha_{e'}}e'\frac{R_d}{A+R_d}\right)}{(\Delta_i - \Delta_{obs})}\frac{A}{C_a}, \quad (6)$$

where a_m (1.8‰) is the discrimination from dissolution and diffusion of CO_2 from the intercellular air spaces to the sites of carboxylation in the chloroplasts.

We evaluated potential measurement artifacts associated with branch excision by comparing A-g_s relationships and g_m/g_s determined from our measurements with those from the literature conducted on intact and excised branches from mature conifer trees in the field (table S1 [tables S1, S2 are available online]; fig. S1 [figs. S1, S2 are available online]). We found little evidence of systematic differences in these relationships due to branch excision, indicating that measurement of photosynthetic gas exchange on excised branches using our approach had no evident impact on the photosynthetic parameters of interest.

A-C_i Response Curves and Relative Limitations of g_s, g_m, and Biochemistry on Photosynthesis

We measured A-C_i response curves for the samples collected in July, August, and September 2015 as described in Monson et al. (2005). We started the measurement sequence with the chamber CO_2 concentration (C_a) of 400 μmol mol^{-1}, then reduced C_a to 200 μmol mol^{-1} for 5 min to stimulate stomatal opening. The assimilation rate was recorded at this value before C_a was reduced to 75 μmol mol^{-1}, followed by incremental increases and measurements at 150, 250, 350, 550, 700, 800, 900, 1200, and 2000 μmol mol^{-1}. The data from the A-C_i responses were used for the limitation analyses.

Quantitative Limitation Analysis

Light-saturated photosynthesis is generally limited by substrate availability and can be expressed as (Farquhar et al. 1980)

$$A_c = \frac{V_{cmax}(C_c - \Gamma^*)}{C_c + K_c(1 + O/K_o)} - R_d, \quad (7)$$

where A_c is the photosynthetic rate at the Rubisco carboxylation-limited stage (μmol CO_2 m^{-2} s^{-1}), V_{cmax} is the maximum rate of Rubisco carboxylation (μmol CO_2 m^{-2} s^{-1}), and C_c (μmol mol^{-1}) and O (210 mmol mol^{-1}) are mole fractions of CO_2 and O_2 at the carboxylation site. Michaelis-Menten constants of Rubisco for CO_2 and O_2 are K_c and K_o, respectively, and R_d is the day respiration rate (μmol CO_2 m^{-2} s^{-1}). The relative changes in light-saturated assimilation rate can be expressed as (Grassi and Magnani 2005)

$$\frac{dA_c}{A_c} = l_s\frac{dg_{sc}}{g_{sc}} + l_m\frac{dg_m}{g_m} + l\frac{dV_{vmax}}{V_{cmax}}, \quad (8)$$

$$l_s = \frac{g_{tot}/g_{sc} \times \partial A/\partial C_c}{g_{tot} + \partial A/\partial C_c}, \quad (9)$$

$$l_m = \frac{g_{tot}/g_m \times \partial A/\partial C_c}{g_{tot} + \partial A/\partial C_c}, \quad (10)$$

$$l_b = \frac{g_{tot}}{g_{tot} + \partial A/\partial C_c}, \quad (11)$$

and

$$\frac{\partial A_c}{\partial C_c} = \frac{V_{cmax}(\Gamma^* + K_c[1 + O/K_o])}{(C_c + K_c[1 + O/K_o])^2}, \quad (12)$$

where l_s, l_m, and l_b are the relative limitations of stomatal conductance to CO_2, mesophyll conductance, and biochemical capacity, respectively. Stomatal conductance to CO_2 is g_{sc} ($g_{sc} = g_s/1.6$). Total conductance to CO_2 between the leaf surface and carboxylation sites is g_{tot} ($1/g_{tot} = 1/g_{sc} + 1/g_m$). To calculate V_{cmax} using the default fitting method (Duursma 2015), A-C_i curves were fitted using the fitacis function with the R package plantecophys. In order to calculate V_{cmax} with respect to C_c ($V_{cmax} - C_c$), g_m was provided as the value measured at a CO_2 concentration of 400 μmol mol^{-1}, assuming a constant value of mesophyll conductance independent of C_a. When estimating V_{cmax} with respect to C_c, the effective Michaelis-Menten constants for CO_2 (K_c) and O_2 (K_o) were assumed to be 260 and 179 μbar, respectively (von Caemmerer et al. 1994; Bahar et al. 2018).

We additionally estimated g_m from A-C_i curves with the method proposed by Ethier and Livingston (2004). Briefly, the response of A to C_i was fitted using the quadratic equation proposed by Ethier and Livingston (2004), which takes into account mesophyll conductance to CO_2.

Leaf Morphology, Nitrogen Content, and Bulk Leaf $\delta^{13}C$ Values

We collected needles following gas exchange and on-line stable isotope discrimination measurements and determined projected leaf area with a flatbed scanner and ImageJ software (http://rsb.info.nih.gov/ij/, US National Institutes of Health). We then dried the leaves for >72 h at 60°C and weighed them for dry mass. We calculated leaf dry mass per area (LMA) from dry mass and the associated projected needle area. We then ground the dried leaf tissue to a fine powder and analyzed the homogenized material for nitrogen elemental concentration and $\delta^{13}C$ values at the University of Wyoming Stable Isotope Facility.

Statistical Analyses

We analyzed the data using a linear mixed effects model for repeated measures to test differences between hillslopes, species, measurement dates, and their interactions for gas exchange parameters and other leaf traits using the R package LME4 (Bates et al. 2015). The fixed effects in the mixed model were hillslope positions, species, measurement dates, and their interactions; the random effect was individual trees, which allowed different intercepts for each plant. Differences in A, g_s, and g_m

between measurement months for a given species and site were evaluated using the least square means pairwise comparisons with the R lsmeans package (Lenth 2016). Linear relationships between related parameters were analyzed using least squares linear regression to evaluate possible correlation between leaf conductance and environmental factors such as soil water content, soil water potentials, leaf morphological traits, and water-use efficiency. All statistical analyses were conducted using R (ver. 3.4.3; R Development Core Team 2017).

Results

Soil Moisture, Temperature, VPD, and Leaf Water Potential

Soil moisture expressed as volumetric soil water content (m^3 m^{-3}) declined at the two hillslope sites from June after snowmelt to September (fig. 1). Soil moisture at a 50-cm depth dropped over this period from 0.32–0.35 to 0.14 m^3 m^{-3} for the two sites. In June, the difference in soil water contents between the two hillslope positions was small. While from July to August the lower hillslope site had higher soil moisture content than the upper hillslope, in September soil moisture at the two hillslope locations converged to the low value of 0.14 m^3 m^{-3} (fig. 1). Daily temperature and VPD were higher at the upper hillslope than at the lower hillslope site over the season (fig. 1).

Average Ψ_{pd} was similar at about −1 MPa for the two species independent of the hillslope position and was insensitive to changes in soil moisture ($P > 0.05$; fig. 2*a*, 2*b*). The Ψ_{md} of *Picea engelmannii* was significantly lower than that of *Pinus contorta* at both hillslope sites in June, August, and September (all $P < 0.05$; fig. 2*c*, 2*d*); for example, in August at the upper hillslope, Ψ_{md} was −2.4 ± 0.3 MPa for *P. engelmannii* and −1.4 ± 0.1 MPa for *P. contorta*. In July, however, the Ψ_{md} values were similar for the two species at the hillslope sites (fig. 2*c*, 2*d*).

Leaf Carbon Isotope Composition, Mass per Area, and Nitrogen Content

We observed no differences in leaf carbon isotope ratios ($\delta^{13}C$) or LMA between the two species or among the four sampling times (mixed effects model, $P > 0.05$; table 2). The leaf nitrogen contents (N%) of *P. contorta* were significantly higher than those of *P. engelmannii* at both study sites and for each sampling time on both mass (N%) and nitrogen per leaf area (NLA) bases (all $P < 0.05$; table 2). But there were no significant differences in N% or NLA between the two study sites or among the four sampling times (all $P > 0.05$; table 2).

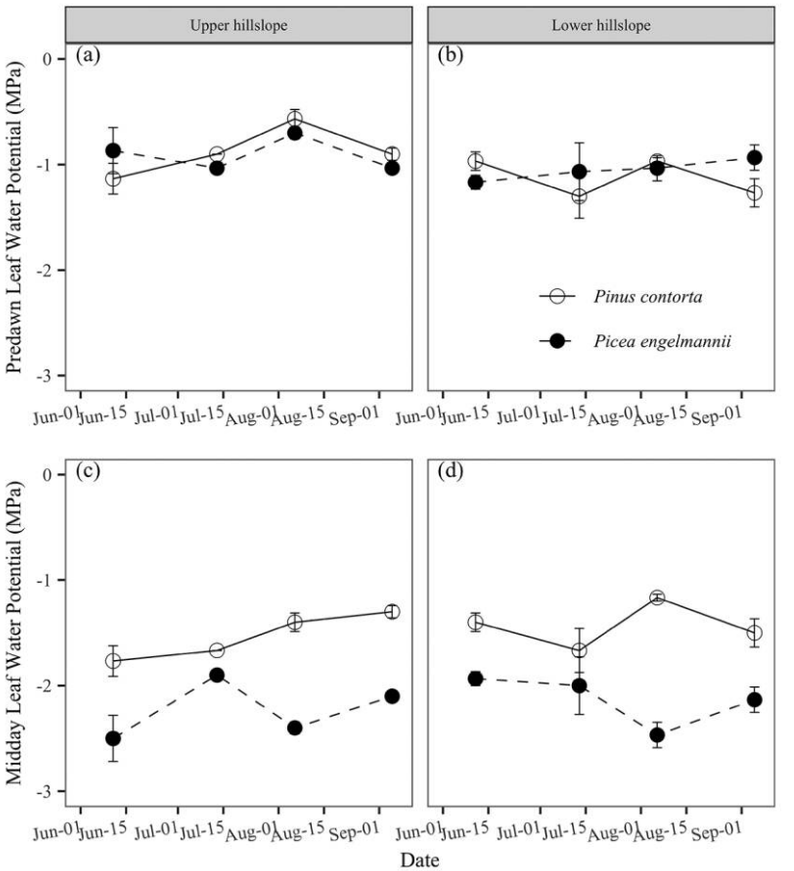

Fig. 2 Predawn and midday water potentials for twigs of the two conifer species at the upper and lower hillslope sites. Values represent the mean ± SE (n = 3).

Table 2

Carbon Isotope Composition of Bulk Leaf Material ($\delta^{13}C$ [‰]), Leaf Mass per Area (LMA), Nitrogen Content (N%), and Nitrogen per Leaf Area (NLA) of Lodgepole Pine (*Pinus contorta*) and Engelmann Spruce (*Picea engelmannii*) at Four Monthly Sampling Periods

Hillslope, species, month	$\delta^{13}C$ (‰)	LMA	N%	NLA (g m^{-2})
Upper hillslope:				
P. contorta:				
June	−27.1 ± .5	390.1 ± 25.5	1.0 ± .05	3.7 ± .1
July	−26.5 ± .4	311.0 ± 37.1	1.1 ± .08	3.5 ± .3
August	−26.3 ± .5	340.0 ± 56.0	1.2 ± .04	4.0 ± .6
September	−26.4 ± .4	328.0 ± 19.1	1.1 ± .08	3.7 ± .4
P. engelmannii:				
June	−26.9 ± .4	384.2 ± 23.0	.7 ± .03	2.8 ± .3
July	−26.4 ± .5	331.2 ± 20.2	.8 ± .05	2.6 ± .1
August	−26.5 ± .2	311.6 ± 11.6	.9 ± .07	2.8 ± .2
September	−27.2 ± .4	330.6 ± 21.8	.9 ± .08	3.0 ± .3
Lower hillslope:				
P. contorta:				
June	−27.1 ± .2	389.5 ± 8.1	1.0 ± .05	3.4 ± .2
July	−27.5 ± .3	334.9 ± 29.9	1.0 ± .08	3.3 ± .6
August	−25.8 ± .5	323.1 ± 33.1	1.2 ± .07	3.8 ± .3
September	−27.0 ± .1	358.4 ± 12.9	1.1 ± .07	4.6 ± 1.5
P. engelmannii:				
June	−26.5 ± .1	410.6 ± 4.9	.7 ± .06	3.0 ± .1
July	−26.7 ± .4	269.8 ± 24.2	.9 ± .09	2.4 ± .1
August	−26.1 ± .5	324.4 ± 12.1	1.0 ± .03	3.1 ± .2
September	−26.9 ± .8	330.6 ± 40.3	.8 ± .04	3.5 ± 1.3

Note. Data are means ± SE (n = 3 or 4).

Net Photosynthetic Rate and Mesophyll and Stomatal Conductances

Photosynthetic rate (A), mesophyll conductance (g_m), and stomatal conductance (g_s) all changed significantly through the growing season as soil moisture decreased at both sites; however, no species effect was observed for A (fig. 3; table 3). In September, A was significantly higher than during the other 3 mo at both sites. In June after snowmelt, A was more than two times higher at the upper hillslope site than at the lower hillslope site ($P < 0.001$; fig. 3*a*, 3*b*; table 3). At the upper hillslope site for *P. contorta* and *P. engelmannii*, A averaged 8.6 ± 1.4 and 7.4 ± 0.5 μmol m^{-2} s^{-1}, respectively. In contrast, A was 3.1 ± 1.1 and 1.7 ± 0.5 μmol m^{-2} s^{-1} for the two species at the lower hillslope site (fig. 3*a*, 3*b*).

There was no significant difference in g_s between the two species or across the hillslope sites (both $P > 0.05$; table 3). However, g_s did change significantly with time at each site, and there were significant interactions between site and measurement time (table 3; fig. 3*c*, 3*d*). At the upper hillslope, g_s was significantly higher in June than in July and August, but in September g_s increased to the same level as in June but with large variations across individuals (fig. 3*c*). At the lower hillslope site, g_s increased from June to September despite declines in soil moisture content over this period (fig. 3*d*). In June, when the soil moisture was ~0.5 m^3 m^{-3}, g_s was significantly higher at the upper hillslope than at the lower hillslope. For *P. contorta* and *P. engelmannii* at the upper hillslope, g_s was 0.100 ± 0.009 and 0.081 ± 0.006 mol m^{-2} s^{-1}, respectively, and was only 0.032 ± 0.006 and 0.014 ± 0.002 mol m^{-2} s^{-1}, respectively, at the lower hillslope (fig. 3*c*, 3*d*). While soil moisture decreased and air temperature increased over the season, g_s gradually increased at the lower hillslope site and decreased at the upper hillslope location, which caused g_s to be significantly higher in August at the lower hillslope compared with the upper hillslope site (fig. 3*c*, 3*d*).

Values of g_m did not differ between the two species (mixed model, $P = 0.112$), but hillslope position had a significant effect on g_m (mixed model, $P = 0.006$; fig. 3*e*, 3*f*). Values of g_m did not differ between the two species at the upper hillslope site at any sampling time (mixed model, $P > 0.05$), while at the lower hillslope site, g_m was significantly higher in *P. engelmannii* than in *P. contorta* in September (Tukey test, $P = 0.003$). At both hillslope positions, g_m increased from June to September, and g_m was significantly higher ($P < 0.05$) in September than during the other 3 mo for *P. engelmannii*, but no significant difference was detected from June to August for *P. contorta* (fig. 3*e*, 3*f*).

Values of A were positively correlated to both g_m and g_s for data pooled across species and hillslope sites (fig. 4*a*, 4*b*), but no correlation was found between g_s and g_m (fig. 4*c*). However, the relationship was stronger between A and g_s than between A and g_m, with 76% of the variation in A explained by g_s, compared with only 21% for g_m.

Values of g_m were negatively correlated with soil moisture at 50-cm depths when the data from both species and two hillslope sites were pooled (fig. 5*a*). However, there was no significant correlation between g_s and soil moisture at 50-cm depths when the data were pooled. Yet there was a negative relationship between g_s and soil moisture content at the lower hillslope site (fig. 5*b*), corresponding to the increase of g_s over the season despite decreasing soil moisture at the lower hillslope. No significant

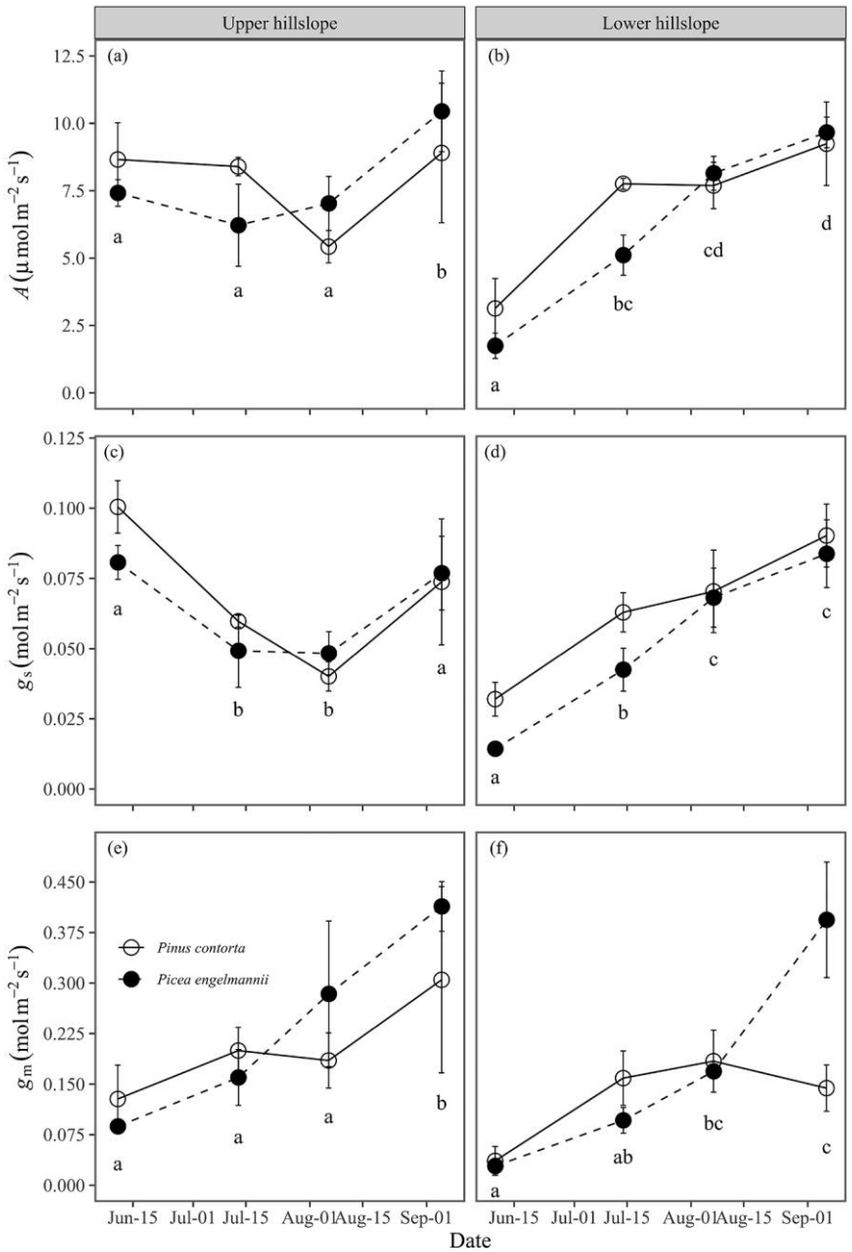

Fig. 3 Average photosynthetic rate (A), stomatal conductance (g_s), and mesophyll conductance (g_m) for the two conifer species at the different hillslope sites. Values are means ± SE (n = 2–4). Different letters beneath the symbols indicate significant differences among sampling campaigns within sites, with data pooled for the two species, which were not significantly different in the ANOVA analysis.

correlation was found between VPD and g_m (fig. 5*c*), while g_m was positively correlated with ambient air temperature (fig. 5*e*). No relationship was found between g_s, VPD, and air temperature (fig. 5*d*, 5*f*).

iWUE did not differ significantly between the upper and lower hillslope sites (fig. 6). iWUE did not change significantly at the lower hillslope over time because of the parallel upscaling of both A and g_s. At the upper hillslope, iWUE increased significantly from June to July for both species because of the significant decrease of g_s/g_m from 0.78 to 0.30 and from 0.92 to 0.22 for *P. contorta* and *P. engelmannnii*, respectively. If pooled together, A/g_s and g_m were also positively correlated (fig. 7).

Limitation of Photosynthesis by g_s, g_m, and Biochemistry

Estimation of the relative limitations of A by g_s, g_m, and biochemistry for the two species at the two hillslope positions from July, August, and September is presented in figure 8. In general, the limitation of photosynthesis caused by g_m was low, ranging from 7% to 18%, which was much less than that imposed by g_s

Table 3

ANOVA Table of the General Linear Mixed Effects Repeated Measures Models for Photosynthetic Rate (*A*), Stomatal Conductance (g_s), and Mesophyll Conductance (g_m) Measured at the Two Hillslope Positions for the Two Species, Lodgepole Pine (*Pinus contorta*) and Engelmann Spruce (*Picea engelmannii*)

		A		g_s		g_m		A/g_s	
	df	*F* value	*P* value	*F* value	*P* value	*F* value	*P* value	*F* value	*P* value
Month	3	15.53	*<.0001*	11.67	*<.0001*	17.89	*<.0001*	11.58	*<.0001*
Site	1	6.95	*.01*	1.54	.23	8.00	*.007*	5.78	*.012*
Species	1	.91	.35	2.29	.15	2.61	.11	4.17	*.046*
Month × site	3	10.52	*<.0001*	23.23	*<.0001*	.23	.87	5.70	*.002*
Month × species	3	3.57	*.02*	1.57	.21	5.55	*.002*	1.81	.16
Site × species	1	.86	.36	.99	.34	*.036*	.851	1.48	.30

(l_s of 42%–67%) and biochemistry (22%–50%; fig. 8). We did not observe any significant effect of hillslope position or species on l_s, l_m, or l_b.

Discussion

Low mesophyll conductance is believed to strongly limit CO_2 assimilation in conifers because, among other factors, needlelike leaves are dense, and their photosynthetic cells have thick cell walls that greatly restrict CO_2 diffusion to chloroplasts (Flexas et al. 2008; Veromann-Jürgenson et al. 2017). However, our measurements of mature field-grown individuals of *Pinus contorta* and *Picea engelmannii* showed that mesophyll conductance was proportionally high and much less of a constraint on CO_2 uptake compared with stomatal conductance. Further, structural investment in leaves, measured as LMA, which has been found to be associated with g_m (Hassiotou et al. 2009), did not differ between the two species or the two hillslope positions, suggesting that structural constraints did not influence variation in g_m for these two conifers. Our results also suggest that as stomatal conductance declined at the upper hillslope, where soil moisture was relatively low and transpiration demand was high from July to August, g_m remained constant and the limitation to photosynthesis imposed by g_m remained relatively stable. Overall, average g_m/g_s values in this study, an index of relative limitations, were all above 1 and increased as soil moisture declined toward the end of the growing season at the comparatively drier upper hillslope site.

Very few studies have reported field measurements of g_m in mature conifer trees, and our estimates of g_m compare well against available data reported by the few studies that used the same ^{13}C discrimination technique (Warren et al. 2003; Bickford et al. 2010; Stangl et al. 2019). On the basis of the available studies of g_m in conifers, the estimations of g_m using the ^{13}C discrimination method generally are higher than those reported in studies using the other methods (Stangl et al. 2019). Indeed, we found our estimates of g_m in conifers to be similar to those reported in studies also using instantaneous ^{13}C discrimination but higher than g_m reported for conifers from studies using curve fitting or the chlorophyll fluorescence methods (table S2). In the current study, we relied on the ^{13}C discrimination method, which may have uncertainties related to the quantities used for isotope fractionations in the model used to estimate g_m (eqq. [3], [6]), such as the fractionations due to diffusion, carboxylation, dark respiration, and photorespiration, and uncertainty in the isotopic signature of the source carbohydrate for respiration (Ubierna and Farquhar 2014; Busch et al. 2020).

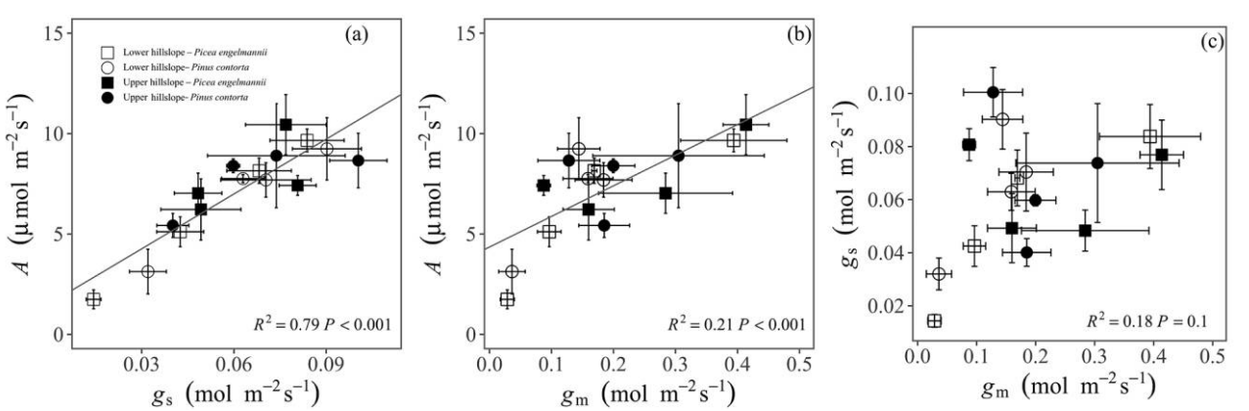

Fig. 4 Correlation between light-saturated photosynthetic rate (*A*) at an ambient intercellular CO_2 concentration (C_a) of 400 μmol mol^{-1} and mesophyll conductance (g_m) and stomatal conductance (g_s), as well as the relationship between g_m and g_s. The lines indicate significant least squares regression relationships for data pooled between species and hillslope sites.

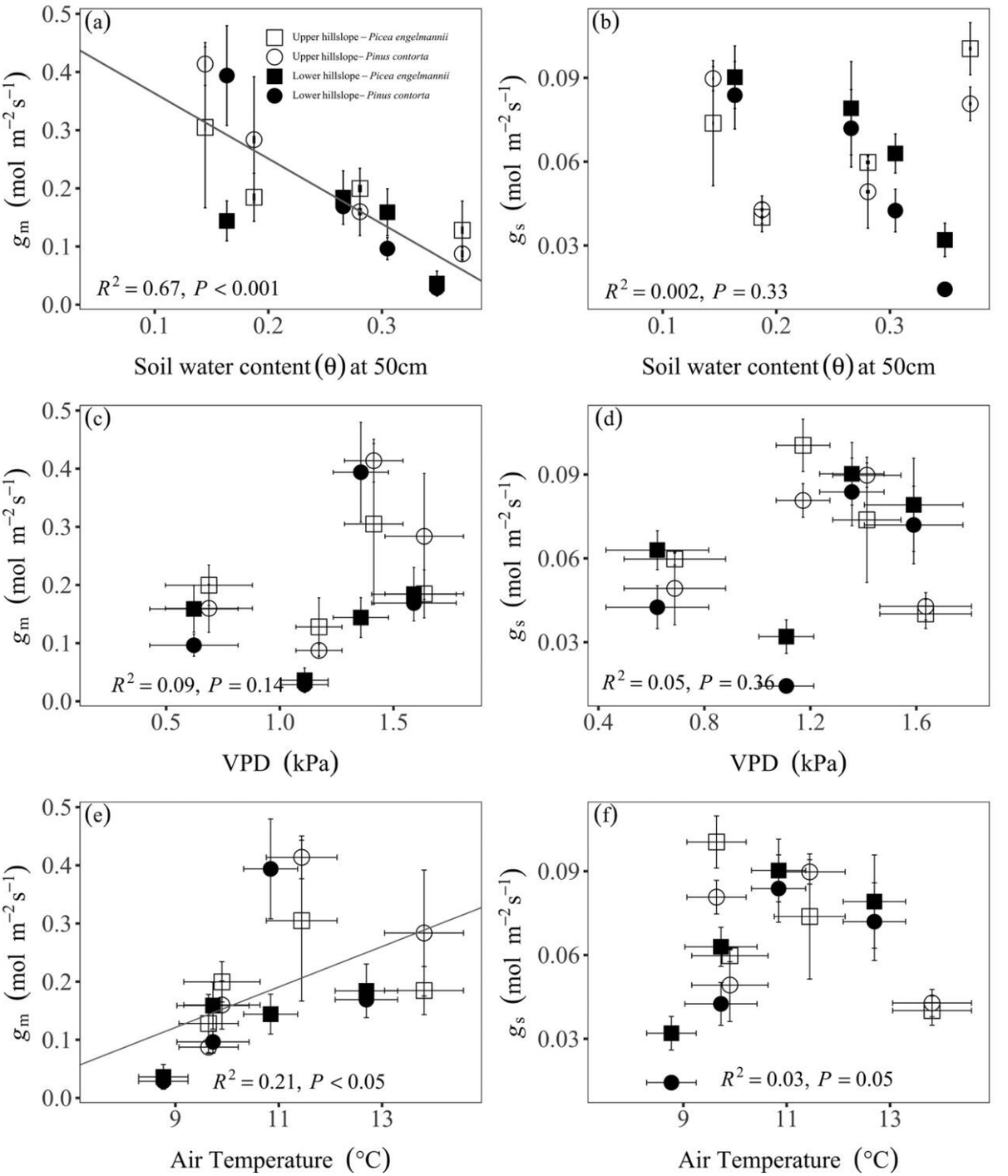

Fig. 5 Relationships of leaf mesophyll conductance (g_m) and stomatal conductance (g_s) to soil moisture, maximum daily vapor pressure deficit (VPD), and daily temperature 7 d before the measurements. The lines indicate significant least squares regression relationships for data pooled between species and hillslope sites.

The potential influence of branch excision on gas exchange characteristics imposes additional uncertainty on the estimates of mesophyll and stomatal conductances in our study. A number of studies have resorted to branch removal and rehydration in the lab to conduct gas exchange measurements on upper-canopy foliage of conifer trees (Monson et al. 2005; Woodruff et al. 2009; Potts et al. 2017), and studies that have directly tested artifacts of branch removal report virtually no impact on gas exchange traits for at least up to 48 h following sample collection from the field (Dang et al. 1997; Richardson and Berlyn 2002;

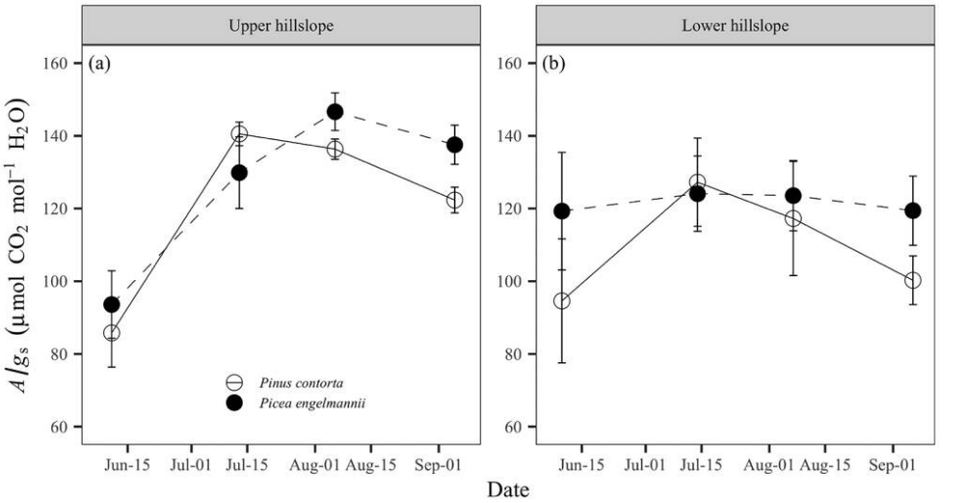

Fig. 6 Intrinsic water use efficiency (photosynthetic rate [A]/stomatal conductance [g_s]) for the two conifer species at the different hillslope sites. Values are means ± SE.

Monson et al. 2005). Our measurements of conifers relating A to g_s in excised branches compare favorably to measurements from other studies that include observations of excised and intact branches (fig. S1), and the modest differences reported across studies could easily be attributed to species' physiological differences or differences in chamber measurement conditions. Thus, we are generally satisfied that any artifacts due to branch excision in our study were minimal.

Considering the caveats noted above, our estimates of g_m and g_s in *P. contorta* and *P. engelmannii* suggest that seasonal environmental changes had contrasting effects on photosynthesis across upper and lower hillslope positions. In the early growing season, the large difference in A and g_s between the upper and lower hillslope sites was due to delayed seasonal recovery of photosynthetic activities at the lower site, which had lower air and soil temperatures. Low soil temperatures impede the rate of spring photosynthetic recovery in conifers (Ensminger et al. 2008; Wu et al. 2013). Reduced soil moisture at the upper hillslope site was associated with a large decline in g_s from June to August but not with g_m or A. We evaluated the relationships between g_s, g_m, soil moisture, daily maximum VPD, and daily air temperature recorded during the week prior to each sampling period. We found that g_m was positively correlated with air temperature, while no relationship was found between g_m and VPD (fig. 5), suggesting that soil moisture availability was likely an overriding factor affecting leaf gas exchange at the upper hillslope site from July to August. At the more mesic lower hillslope site, g_s, g_m, and A increased despite the seasonal decline in soil moisture content. Surprisingly, no relationship was found between g_s and VPD when the data were pooled together from the two hillslope locations (fig. 5*d*). Further, reductions in g_s, but not g_m and A, demonstrate that maintenance of sufficient mesophyll conductance may have an important role in sustaining the photosynthetic rate independent of g_s, which is supported further by the correlation between A and g_m but the lack of correlation between g_m and g_s. The high A, g_s, and g_m values in September despite the continued decline in soil moisture content suggest that gas exchange may have been regulated by interactions among soil moisture, air temperature, and VPD. The evaporation demand was low in September, as indicated by VPD. The idea that changes in mesophyll conductance could potentially play an important independent role in controlling photosynthetic responses to soil water limitation has been recognized (Niinemets et al. 2009; Keenan et al. 2010; Gago et al. 2019). Previous studies, including experimental work on conifer seedlings, found that rapidly imposed reductions in soil water supply often led to

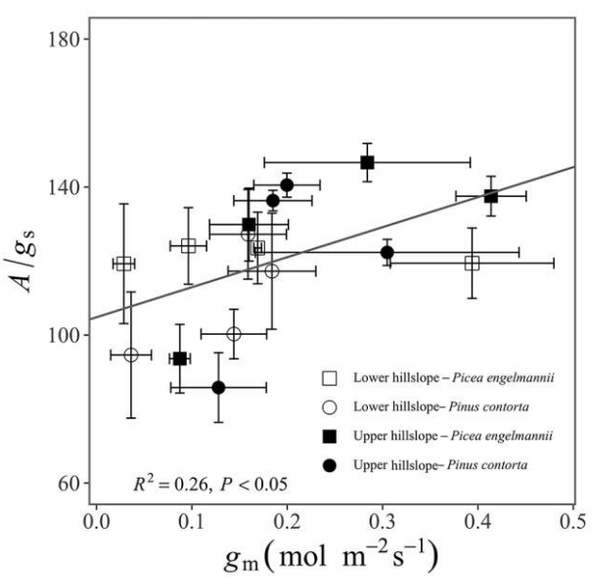

Fig. 7 Correlation between intrinsic water use efficiency (photosynthetic rate [A]/stomatal conductance [g_s]) and leaf mesophyll conductance (g_m). The lines indicate significant least squares regression relationships for data pooled between species and hillslope sites.

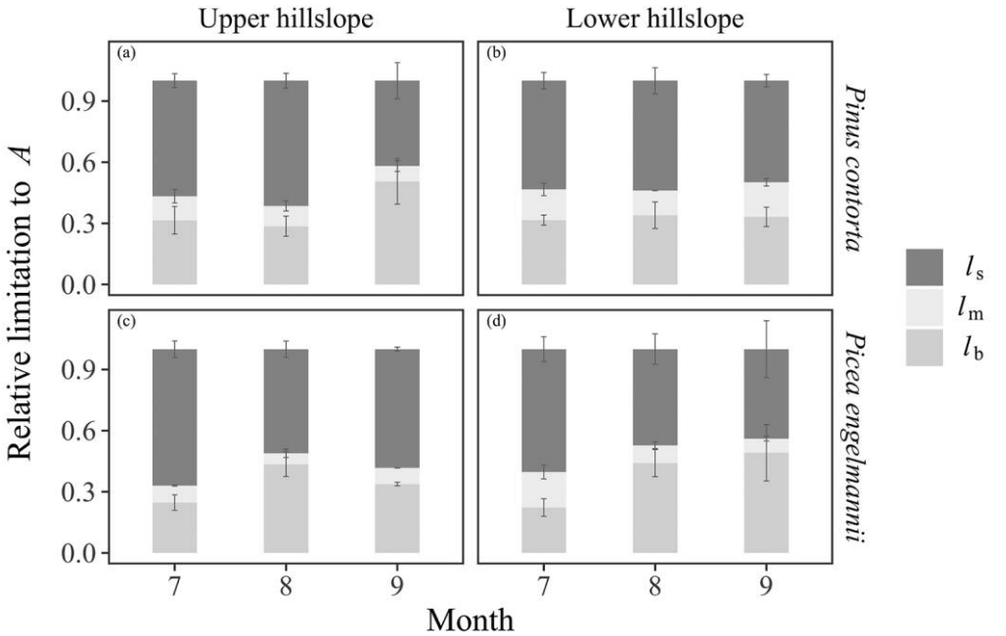

Fig. 8 Relative limitations to the CO_2 assimilation rate (A) by stomatal conductance (l_s), mesophyll conductance (l_m), and biochemistry (l_b) for the two species at the upper and lower hillslopes. Data are presented as means ± SE.

reduced g_m (Galmés et al. 2007; Duan et al. 2011). Conversely, the g_m of black spruce seedlings did not respond to multiple cycles of drought, although g_s was significantly reduced by drought treatments (Stewart et al. 1995). It is well known that stomatal conductance decreases with declines in soil water availability (Lawlor and Cornic 2002), but the responses of mesophyll conductance to long-term water deficits are still uncertain. In some species, stomatal closure played by far the main role in the decline of photosynthesis under moderate water stress (Chaves et al. 2009), but shifts in mesophyll conductance may also play a central role in some instances (Flexas et al. 2002; Galmés et al. 2007). In our study, we conclude that stomatal conductance was the main limitation to photosynthesis, suggesting that productivity was heavily constrained by stomatal closure in response to differences in water limitation or energy balance and temperatures across the hillslope positions, at least at the relatively xeric upper hillslope site. Similar results were found in a study where *Eucalyptus* acclimated to slowly induced long-term water stress, which led to reduced g_m limitation (Cano et al. 2014). The central Rocky Mountain region is characterized by heavy winter and spring snowfall and dry summers, such that local plant communities often experience water stress late in the growing season, especially at sites on exposed south-facing slopes and where soil depth is shallow. Within such environments, sustaining proportionally high values of mesophyll conductance could potentially allow conifers to cope with prolonged water limitations during the growing season.

We observed little variation in predawn and midday leaf water potential despite 50% reductions in stomatal conductance at the upper hillslope site from July to August, suggesting that predawn and midday water potentials were not useful indicators of water limitation in these two species. Besides the soil water content differences, temperature and VPD differed between the upper and lower hillslope positions. Values of g_m were positively correlated with temperature, which is consistent with previous studies that investigated the relationship between temperature and g_m under controlled settings (Bernacchi et al. 2002; Scafaro et al. 2011; Evans and von Caemmerer 2013; von Caemmerer and Evans 2015). No relationship between VPD and g_m was observed. A few other studies have also found that VPD had no significant impact on g_m (Warren 2008*a*; Stangl et al. 2019). The negative correlation between g_m and soil water content might not have direct causality, as temperature increased when soil moisture decreased. As such, it is difficult to untangle the roles of temperature and soil water content in adjustments in g_m, especially at the lower hillslope location. The results suggest that the interaction of air temperature and soil water availability drives differences in mesophyll conductance across the complex hillslope gradient within our study.

Adjustments in g_m independent of g_s also strongly influenced iWUE (iWUE = A/g_s) in the two conifers studied here, as indicated by a positive correlation between A and g_m and no correlation between g_m and g_s. This confirms the prevailing assumption that enhancing g_m will improve iWUE (Flexas et al. 2013*a*, 2016). A meta-analysis study of multiple species has also detected no relationship between g_m and g_s (Gago et al. 2016), which indicates possible decoupling of g_s and g_m in regulating iWUE under different environmental conditions. We did not measure or model in situ transpiration rates in the current study, but if leaf to air vapor pressure gradients were similar across the two species and hillslope environments, the positive correlation between g_m and A/g_s would also extend to a positive correlation between g_m and A/E. We hypothesize, therefore, that seasonal enhancement of g_m with decreasing soil moisture or increases in seasonal

temperature could increase plant productivity relative to water loss in Rocky Mountain conifers, at least at the leaf level.

Contrary to our expectation that the isohydric *P. contorta* and the anisohydric *P. engelmannii* would exhibit contrasting responses of mesophyll conductance to soil water limitation, the two species had similar g_m values and responses over the growing season at the two hillslope sites (fig. 3; table 2). Tighter control of stomata in *P. contorta* was not accompanied by a higher mesophyll conductance to compensate for the early closure of stomata during water stress compared with *P. engelmannii*. At the upper hillslope site, stomatal conductance was reduced late in the season to maintain minimum midday leaf water potentials, while at the lower hillslope site, soil water availability was apparently high enough to support an increase of stomatal conductance for both species as temperatures warmed during the growing season. We speculate that in the conifers we studied, g_s and g_m might be influenced by different mechanisms. Given the coupled pathways for water and CO_2 exchange, g_m might be more closely coordinated with leaf hydraulic conductance and photosynthetic capacity. Flexas et al. (2013*b*) found a strong correlation between A and g_m across diverse species and suggested that mesophyll structural and physiological traits that control g_m also influence leaf hydraulics. We did not investigate relationships between leaf hydraulic properties and g_m in our study but acknowledge the importance of functional integration between these traits, warranting further study.

To our surprise, g_m did not impose the greatest limitation on photosynthesis in the two conifers. Despite some uncertainties involved with g_m estimation, the limitation on photosynthesis imposed by mesophyll conductance in this study was less than one-third the limitation imposed by stomata (fig. 8). Maintaining a high g_m is beneficial to plants that experience water shortage because it can increase photosynthesis without increasing transpiration (Flexas et al. 2008). This is consistent with the correlation between g_m and A and A/g_s. Few studies have investigated the g_m limitation of A in conifers, but of those, several have determined that g_m was less limiting for A than g_s was (Warren et al. 2003; Peguero-Pina et al. 2012). In contrast, a few other available studies show that the limitation on A imposed by g_m was larger than that of g_s (Stewart et al. 1995; De Lucia et al. 2003; Peguero-Pina et al. 2012). The divergence could be attributed to optimization differences across species. Veromann-Jürgenson et al. (2017) summarized all the available data on g_m in 13 conifer species and found that variation in g_m was high. One highlighted trait suggested to be a strong factor in determining g_m is chloroplast surface area exposed to intercellular air space (S_c/S), which changes as environmental conditions change (Evans et al. 2009; Tomás et al. 2013; Evans 2021). In this study, we found that mesophyll conductance (g_m) overall imposed a small limitation on photosynthesis, but key adjustments in this trait played an important role in sustaining photosynthesis when stomatal conductance decreased with water limitation. To more broadly understand the role of g_m in limiting A in conifers, quantification of g_m for many other conifer species under contrasting field conditions is required.

Acknowledgments

We thank Evan Kipnis for his assistance with fieldwork and Chris Feng for comments on this article. We also thank the staff members of the Stable Isotope Facility at the University of Wyoming for assistance with stable isotope analysis and Heather Speckman for providing soil moisture, air temperature, and humidity data. J. Guo, D. G. Williams, and B. E. Ewers conceived and designed the experiments, J. Guo and D. P. Beverly performed the experiments, and C. S. Cook provided help on stable isotope analyses. J. J. Mercer provided assistance with data analysis and detailed feedback related to the manuscript. J. Guo and D. G. Williams analyzed the data and wrote the manuscript, and all authors provided feedback on the manuscript before submission. The data that support the findings of this study are openly available at WyoScholar, a repository service that collects, preserves, and provides access to research data from the University of Wyoming. The data are indexed at https://doi.org/10.15786/16920139.v1. We declare that we have no conflict of interest. This work was supported by the National Science Foundation under award EPS-1208909.

Literature Cited

Bahar NHA, L Hayes, AP Scafaro, OK Atkin, JR Evans 2018 Mesophyll conductance does not contribute to greater photosynthetic rate per unit nitrogen in temperate compared with tropical evergreen wet-forest tree leaves. New Phytol 218:492–505.

Barbour MM, JR Evans, KA Simonin, S von Caemmerer 2016 Online CO_2 and H_2O oxygen isotope fractionation allows estimation of mesophyll conductance in C_4 plants, and reveals that mesophyll conductance decreases as leaves age in both C_4 and C_3 plants. New Phytol 210:875–889.

Barbour MM, CR Warren, GD Farquhar, GUY Forrester, H Brown 2010 Variability in mesophyll conductance between barley genotypes, and effects on transpiration efficiency and carbon isotope discrimination. Plant Cell Environ 33:1176–1185.

Bates D, M Mächler, B Bolker, S Walker 2015 Fitting linear mixed-effects models using lme4. J Stat Softw 67:1–48.

Bernacchi CJ, AR Portis, H Nakano, S von Caemmerer, SP Long 2002 Temperature response of mesophyll conductance: implications for the determination of Rubisco enzyme kinetics and for limitations to photosynthesis in vivo. Plant Physiol 130:1992–1998.

Bickford CP, DT Hanson, NG McDowell 2010 Influence of diurnal variation in mesophyll conductance on modelled ^{13}C discrimination: results from a field study. J Exp Bot 61:3223–3233.

Bickford CP, NG Mcdowell, EB Erhardt, DT Hanson 2009 High-frequency field measurements of diurnal carbon isotope discrimination and internal conductance in a semi-arid species, *Juniperus monosperma*. Plant Cell Environ 32:796–810.

Bonan GB 2019 Climate change and terrestrial ecosystem modeling. Cambridge University Press, Cambridge.

Brodribb TJ, NM Holbrook 2003 Stomatal closure during leaf dehydration, correlation with other leaf physiological traits. Plant Physiol 132:2166–2173.

Buckley TN 2005 The control of stomata by water balance. New Phytol 168:275–292.

Busch FA, M Holloway-Phillips, H Stuart-Williams, GD Farquhar 2020 Revisiting carbon isotope discrimination in C_3 plants shows respiration rules when photosynthesis is low. Nat Plants 6:245–258.

Cano FJ, R López, CR Warren 2014 Implications of the mesophyll conductance to CO_2 for photosynthesis and water-use efficiency

during long-term water stress and recovery in two contrasting eucalyptus species. Plant Cell Environ 37:2470–2490.

Cano FJ, D Sánchez-Gómez, J Rodríguez-Calcerrada, CR Warren, L Gil, I Aranda 2013 Effects of drought on mesophyll conductance and photosynthetic limitations at different tree canopy layers. Plant Cell Environ 36:1961–1980.

Cernusak LA, N Ubierna, K Winter, JA Holtum, JD Marshall, GD Farquhar 2013 Environmental and physiological determinants of carbon isotope discrimination in terrestrial plants. New Phytol 200:950–965.

Chaves MM, J Flexas, C Pinheiro 2009 Photosynthesis under drought and salt stress: regulation mechanisms from whole plant to cell. Ann Bot 103:551–560.

Dang Q-L, HA Margolis, MR Coyea, M Sy, GJ Collatz 1997 Regulation of branch-level gas exchange of boreal trees: roles of shoot water potential and vapor pressure difference. Tree Physiol 17:521–535.

De Lucia EH, D Whitehead, MJ Clearwater 2003 The relative limitation of photosynthesis by mesophyll conductance in co-occurring species in a temperate rainforest dominated by the conifer *Dacrydium cupressinum*. Funct Plant Biol 30:1197–1204.

Dewar R, A Mauranen, A Mäkelä, T Hölttä, B Medlyn, T Vesala 2018 New insights into the covariation of stomatal, mesophyll and hydraulic conductances from optimization models incorporating nonstomatal limitations to photosynthesis. New Phytol 217:571–585.

Duan B, F Ran, X Zhang, Y Zhang, H Korpelainen, C Li 2011 Long-term acclimation of mesophyll conductance, carbon isotope discrimination and growth in two contrasting *Picea asperata* populations exposed to drought and enhanced UV-B radiation for three years. Agric For Meteorol 151:116–126.

Duursma RA 2015 Plantecophys—an R package for analysing and modelling leaf gas exchange data. PLoS ONE 10:e0143346.

Ensminger I, L Schmidt, J Lloyd 2008 Soil temperature and intermittent frost modulate the rate of recovery of photosynthesis in Scots pine under simulated spring conditions. New Phytol 177:428–442.

Ethier G, N Livingston 2004 On the need to incorporate sensitivity to CO_2 transfer conductance into the Farquhar–von Caemmerer–Berry leaf photosynthesis model. Plant Cell Environ 27:137–153.

Evans JR 2021 Mesophyll conductance: walls, membranes and spatial complexity. New Phytol 229:1864–1876.

Evans JR, R Kaldenhoff, B Genty, I Terashima 2009 Resistances along the CO_2 diffusion pathway inside leaves. J Exp Bot 60:2235–2248.

Evans JR, T Sharkey, J Berry, G Farquhar 1986 Carbon isotope discrimination measured concurrently with gas exchange to investigate CO_2 diffusion in leaves of higher plants. Funct Plant Biol 13:281–292.

Evans JR, S von Caemmerer 1996 Carbon dioxide diffusion inside leaves. Plant Physiol 110:339–346.

——— 2013 Temperature response of carbon isotope discrimination and mesophyll conductance in tobacco. Plant Cell Environ 36:745–756.

Farquhar GD, LA Cernusak 2012 Ternary effects on the gas exchange of isotopologues of carbon dioxide. Plant Cell Environ 35:1221–1231.

Farquhar GD, R Richards 1984 Isotopic composition of plant carbon correlates with water-use efficiency of wheat genotypes. Funct Plant Biol 11:539–552.

Farquhar GD, S von Caemmerer, J Berry 1980 A biochemical model of photosynthetic CO_2 assimilation in leaves of C_3 species. Planta 149:78–90.

Flexas J, MM Barbour, O Brendel, HM Cabrera, M Carriquí, A Díaz-Espejo, C Douthe, E Dreyer, JP Ferrio, J Gago 2012 Mesophyll diffusion conductance to CO_2: an unappreciated central player in photosynthesis. Plant Sci 193:70–84.

Flexas J, J Bota, JM Escalona, B Sampol, H Medrano 2002 Effects of drought on photosynthesis in grapevines under field conditions: an evaluation of stomatal and mesophyll limitations. Funct Plant Biol 29:461–471.

Flexas J, A Díaz-Espejo, MA Conesa, RE Coopman, C Douthe, J Gago, A Gallé, et al 2016 Mesophyll conductance to CO_2 and Rubisco as targets for improving intrinsic water use efficiency in C_3 plants. Plant Cell Environ 39:965–982.

Flexas J, Ü Niinemets, A Gallé, MM Barbour, M Centritto, A Diaz-Espejo, C Douthe, J Galmés, M Ribas-Carbo, PL Rodriguez 2013*a* Diffusional conductances to CO_2 as a target for increasing photosynthesis and photosynthetic water-use efficiency. Photosynth Res 117:45–59.

Flexas J, M Ribas-Carbó, A Diza-Espejo, J Galmés, H Medrano 2008 Mesophyll conductance to CO_2: current knowledge and future prospects. Plant Cell Environ 31:602–621.

Flexas J, C Scoffoni, J Gago, L Sack 2013*b* Leaf mesophyll conductance and leaf hydraulic conductance: an introduction to their measurement and coordination. J Exp Bot 64:3965–3981.

Gago J, M Carriquí, M Nadal, MJ Clemente-Moreno, RE Coopman, AR Fernie, J Flexas 2019 Photosynthesis optimized across land plant phylogeny. Trends Plant Sci 24:947–958.

Gago J, D de Menezes Daloso, CM Figueroa, J Flexas, AR Fernie, Z Nikoloski 2016 Relationships of leaf net photosynthesis, stomatal conductance, and mesophyll conductance to primary metabolism: a multispecies meta-analysis approach. Plant Physiol 171:265–279.

Galmés J, H Medrano, J Flexas 2007 Photosynthetic limitations in response to water stress and recovery in Mediterranean plants with different growth forms. New Phytol 175:81–93.

Grassi G, F Magnani 2005 Stomatal, mesophyll conductance and biochemical limitations to photosynthesis as affected by drought and leaf ontogeny in ash and oak trees. Plant Cell Environ 28:834–849.

Hassiotou F, M Ludwig, M Renton, EJ Veneklaas, JR Evans 2009 Influence of leaf dry mass per area, CO_2, and irradiance on mesophyll conductance in sclerophylls. J Exp Bot 60:2303–2314.

Keenan T, S Sabate, C Gracia 2010 Soil water stress and coupled photosynthesis–conductance models: bridging the gap between conflicting reports on the relative roles of stomatal, mesophyll conductance and biochemical limitations to photosynthesis. Agric For Meteorol 150:443–453.

Kooijmans LMJ, W Sun, J Aalto, K-M Erkkilä, K Maseyk, U Seibt, T Vesala, I Mammarella, H Chen 2019 Influences of light and humidity on carbonyl sulfide-based estimates of photosynthesis. Proc Natl Acad Sci USA 116:2470–2475.

Lawlor DW, G Cornic 2002 Photosynthetic carbon assimilation and associated metabolism in relation to water deficits in higher plants. Plant Cell Environ 25:275–294.

Lenth RV 2016 Least-squares means: the R package lsmeans. J Stat Softw 69:1–33.

McDowell N, WT Pockman, CD Allen, DD Breshears, N Cobb, T Kolb, J Plaut, et al 2008 Mechanisms of plant survival and mortality during drought: why do some plants survive while others succumb to drought? New Phytol 178:719–739.

Monson RK, JP Sparks, TN Rosenstiel, LE Scott-Denton, TE Huxman, PC Harley, AA Turnipseed, SP Burns, B Backlund, J Hu 2005 Climatic influences on net ecosystem CO_2 exchange during the transition from wintertime carbon source to springtime carbon sink in a high-elevation, subalpine forest. Oecologia 146:130–147.

Niinemets Ü, A Díaz-Espejo, J Flexas, J Galmés, CR Warren 2009 Role of mesophyll diffusion conductance in constraining potential photosynthetic productivity in the field. J Exp Bot 60:2249–2270.

Ogée J, L Wingate, B Genty 2018 Estimating mesophyll conductance from measurements of $C^{18}OO$ photosynthetic discrimination and carbonic anhydrase activity. Plant Physiol 178:728–752.

Peguero-Pina JJ, J Flexas, J Galmés, Ü Niinemets, D Sancho-Knapik, G Barredo, D Villarroya, E Gil-Pelegrín 2012 Leaf anatomical properties in relation to differences in mesophyll conductance to CO_2 and photosynthesis in two related Mediterranean *Abies* species. Plant Cell Environ 35:2121–2129.

Potts DL, RL Minor, Z Braun, GA Barron-Gafford 2017 Photosynthetic phenological variation may promote coexistence among codominant tree species in a Madrean sky island mixed conifer forest. Tree Physiol 37:1229–1238.

R Development Core Team 2017 R: a language and environment for statistical computing. R Foundation for Statistical Computing, Vienna.

Richardson AD, GP Berlyn 2002 Changes in foliar spectral reflectance and chlorophyll fluorescence of four temperate species following branch cutting. Tree Physiol 22:499–506.

Roeske CA, MH O'Leary 1984 Carbon isotope effects on enzyme-catalyzed carboxylation of ribulose bisphosphate. Biochemistry 23:6275–6284.

Scafaro AP, S von Caemmerer, JR Evans, BJ Atwell 2011 Temperature response of mesophyll conductance in cultivated and wild *Oryza* species with contrasting mesophyll cell wall thickness. Plant Cell Environ 34:1999–2008.

Sevanto S, M Ryan, LT Dickman, D Derome, A Patera, T Defraeye, RE Pangle, PJ Hudson, WT Pockman 2018 Is desiccation tolerance and avoidance reflected in xylem and phloem anatomy of two coexisting arid-zone coniferous trees? Plant Cell Environ 41:1551–1564.

Sperry JS 2000 Hydraulic constraints on plant gas exchange. Agric For Meteorol 104:13–23.

Stangl ZR, L Tarvainen, G Wallin, N Ubierna, M Räntfors, JD Marshall 2019 Diurnal variation in mesophyll conductance and its influence on modelled water-use efficiency in a mature boreal *Pinus sylvestris* stand. Photosynth Res 141:53–63.

Stewart JD, AZ El Abidine, PY Bernier 1995 Stomatal and mesophyll limitations of photosynthesis in black spruce seedlings during multiple cycles of drought. Tree Physiol 15:57–64.

Tazoe Y, S von Caemmerer, GM Estavillo, JR Evans 2011 Using tunable diode laser spectroscopy to measure carbon isotope discrimination and mesophyll conductance to CO_2 diffusion dynamically at different CO_2 concentrations. Plant Cell Environ 34:580–591.

Thayer D, AD Parsekian, K Hyde, H Speckman, D Beverly, B Ewers, M Covalt, et al 2018 Geophysical measurements to determine the hydrologic partitioning of snowmelt on a snow-dominated subalpine hillslope. Water Resour Res 54:3788–3808.

Tomás M, J Flexas, L Copolovici, J Galmés, L Hallik, H Medrano, M Ribas-Carbó, T Tosens, V Vislap, Ü Niinemets 2013 Importance of leaf anatomy in determining mesophyll diffusion conductance to CO_2 across species: quantitative limitations and scaling up by models. J Exp Bot 64:2269–2281.

Tholen D, X-G Zhu 2011 The mechanistic basis of internal conductance: a theoretical analysis of mesophyll cell photosynthesis and CO_2 diffusion. Plant Physiol 156:90–105.

Ubierna N, GD Farquhar 2014 Advances in measurements and models of photosynthetic carbon isotope discrimination in C_3 plants. Plant Cell Environ 37:1494–1498.

Ubierna N, JD Marshall 2011 Estimation of canopy average mesophyll conductance using $\delta^{13}C$ of phloem contents. Plant Cell Environ 34:1521–1535.

Veromann-Jürgenson L-L, TJ Brodribb, Ü Niinemets, T Tosens 2020 Variability in the chloroplast area lining the intercellular airspace and cell walls drives mesophyll conductance in gymnosperms. J Exp Bot 71:4958–4971.

Veromann-Jürgenson L-L, T Tosens, L Laanisto, Ü Niinemets 2017 Extremely thick cell walls and low mesophyll conductance: welcome to the world of ancient living! J Exp Bot 68:1639–1653.

von Caemmerer S, JR Evans 2015 Temperature responses of mesophyll conductance differ greatly between species. Plant Cell Environ 38:629–637.

von Caemmerer S, JR Evans, GS Hudson, TJ Andrews 1994 The kinetics of ribulose-1,5-bisphosphate carboxylase/oxygenase in vivo inferred from measurements of photosynthesis in leaves of transgenic tobacco. Planta 195:88–97.

von Caemmerer S, GD Farquhar 1981 Some relationships between the biochemistry of photosynthesis and the gas exchange of leaves. Planta 153:376–387.

Warren CR 2008*a* Soil water deficits decrease the internal conductance to CO_2 transfer but atmospheric water deficits do not. J Exp Bot 59:327–334.

——— 2008*b* Stand aside stomata, another actor deserves centre stage: the forgotten role of the internal conductance to CO_2 transfer. J Exp Bot 59:1475–1487.

Warren CR, G Ethier, N Livingston, N Grant, D Turpin, D Harrison, T Black 2003 Transfer conductance in second growth Douglas-fir (*Pseudotsuga menziesii* (Mirb.) Franco) canopies. Plant Cell Environ 26:1215–1227.

Wingate L, U Seibt, JB Moncrieff, PG Jarvis, J Lloyd 2007 Variations in ^{13}C discrimination during CO_2 exchange by *Picea sitchensis* branches in the field. Plant Cell Environ 30:600–616.

Woodruff DR, FC Meinzer, B Lachenbruch, DM Johnson 2009 Coordination of leaf structure and gas exchange along a height gradient in a tall conifer. Tree Physiol 29:261–272.

Woodward FI 1995 Ecophysiological controls of conifer distributions. Pages 79–94 *in* WK Smith, TM Hinckley, eds. Ecophysiology of coniferous forests. Academic Press, San Diego, CA.

Wu J, D Guan, F Yuan, A Wang, C Jin 2013 Soil temperature triggers the onset of photosynthesis in Korean pine. PloS ONE 8:e65401.